National Defence / Défense nationale

A THEORETICAL MODEL FOR AIRBORNE RADARS

by

D. Faubert
Airborne Radar Section
Radar Division

DEFENCE RESEARCH ESTABLISHMENT OTTAWA
REPORT NO. 1017

PCN
21LA12

November 1989
Ottawa

90-03931/

ABSTRACT

This work describes a theoretical model for the simulation of airborne (or spaceborne) radars. This model can be used to simulate many types of systems including Airborne Intercept and Airborne Early Warning radars, Airborne Missile Approach Warning Systems etc. We derive a theoretical expression for the average Signal–to–Noise ratio at the output of the signal processor. This can be used to obtain the average performance of the radar without employing Monte Carlo techniques. The model makes provision for a waveform without frequency modulation and for one with linear frequency modulation. The waveform may also use frequency hopping for Electronic Counter Counter Measures or for clutter suppression. The model can accommodate any type of encounter including air–to–air, air–to–ground (look–down) and rear attacks. It can simulate systems with multiple phase centers on receive for studying advanced clutter or jamming interference suppression techniques. To demonstrate the validity and the capability of the model, a baseline Airborne Intercept radar system is simulated.

RÉSUMÉ

Ce travail décrit un modèle théorique pour la simulation des radars aéroportés (ou déployés dans l'espace). On peut l'utiliser pour simuler plusieurs genres de systèmes incluant les radars d'interception aérienne, les radars de veille à longue portée, les systèmes de surveillance d'attaque par missiles etc. Le modèle calcule le rapport signal sur bruit moyen du système après traitement du signal. Il peut simuler une onde porteuse sans modulation de fréquence ou avec modulation linéaire de la fréquence. L'onde porteuse peut changer de fréquence périodiquement pour tirer avantage des techniques de contre–contre mesures électroniques ou de réduction du clutter. Le modèle s'applique à des engagements air–air, air–sol et d'attaque par l'arrière. Il peut décrire des récepteurs ayant plusieurs centres de phase. Ce genre de récepteur est quelques fois utilisé pour réduire l'interférence causé par le clutter ou le brouillage électronique. On présente quelques résultats ayant trait à un radar d'interception aérienne pour démontrer l'utilité et la validité du modèle.

EXECUTIVE SUMMARY

The requirement for evaluating the performance of airborne radars often arises in the Department of National Defense. This report is the outcome of an effort to develop a general purpose model for the simulation of these systems. It can be used to study multi–mode Airborne Intercept radars (AI) deployed on–board high performance fighter aircraft, Missile Approach Warning Systems deployed on helicopters, propeller and jet aircraft, Airborne Early Warning radars deployed on surveillance aircraft like the AWACS, etc. The model also applies for Space Based Radars (SBRs).

In the theory, we derive expressions for the signals found in the radar receiver. Hence with minor modifications, the model could be used to generate signals for input to a real radar signal processor.

To ensure the widest possible applicability, the model accounts for various system configurations. It has provision for various types of waveforms. The radar carrier frequency can also change periodically to counter jamming or to reduce clutter interference. The model also applies to radars equipped with more than one antenna, as radars of this type perform better in the presence of jamming and clutter. Finally, the model geometry accommodates air–to–air, air–to–ground and rear–attack encounters.

The first part of the report contains the equations for the signal received from a point target. The signal from a distributed target, like ground clutter, is an extension of the expressions for the point target. The calculations also deal with the contribution of the receiver thermal noise. Finally, an expression for the average value of the combined interference of clutter and noise is derived. This allows the evaluation of the average performance of the radar without using time–consuming Monte Carlo techniques.

A baseline radar system serves as a test bed to demonstrate the validity and the capability of the theory. The model highlights the impact of clutter and white thermal noise on target detection.

The model has a wide range of applications for DND. It could be used to evaluate Airborne Intercept and Airborne Early Warning radars, Missile Approach Warning Systems etc. It is also of interest to the TTCP Panel KTP–5 which is concerned with the detection of low radar cross section targets.

TABLE OF CONTENTS

		Page
Abstract		iii
Résumé		iii
Executive Summary		v
Table of contents		vii
List of figures		ix
List of tables		ix
1.0	INTRODUCTION	1
2.0	THEORETICAL MODEL	1
2.1	The Geometry	4
2.2	The Propagation Delay	5
2.3	The Transmitted Radar Signal	13
2.4	The Signal from a Point Source	15
	2.4.1 The NFM Waveform	22
	2.4.2 The LFM Waveform	28
2.5	The Signal from a Distributed Target	36
2.6	The Clutter Covariance Matrix	38
2.7	The Thermal Noise Covariance Matrix	39
2.8	The Signal–to–Interference Ratio	42
3.0	NUMERICAL RESULTS	43
3.1	The Computer Simulation	43
3.2	The Baseline Airborne Radar System	43
4.0	CONCLUSION	50
5.0	REFERENCES	50
Table of symbols		53

LIST OF FIGURES

Figure		Page
1	Geometry of the problem	5
2	Location of the phase centers and the target	12
3	Radar system block diagram	16
4	Diagram showing the transmitted and the received waveforms	17
5	Integration limits for the NFM waveform	25
6	The Signal–to–Interference Ratio for the baseline system	46
7	SIR of the baseline system with altitude return	47
8	SIR of the LFM and NFM "equivalent" waveform	48
9	SIR of the baseline system for an air–to–air encounter	49

LIST OF TABLES

Table		Page
I	Airborne radar simulator options	2
II	Worst case values for ABR calculations	8
III	Airborne Intercept radar parameters	44

1.0 INTRODUCTION

Modern military aircraft make extensive use of radar systems for target acquisition. As an example, the Canadian CF–18 aircraft is equipped with the Hughes AN/APG–65 coherent radar. It uses pulse Doppler techniques to counter clutter and jamming. This multi–mode Airborne Intercept (AI) radar can operate in a number of ways to deal with a wide variety of targets under various operational conditions. The importance of radars in many airborne weapon systems used by the Canadian Forces dictates a detailed understanding of their operation and capabilities.

In support of the Canadian Forces (CF), the Radar Division of DREO is studying airborne radar systems under Tasks DFTEM–102. This report describes the first phase of this work consisting in modeling the operation of airborne radars.

Section 2.0 derives the airborne radar model. Section 3.0 describes the computer simulation implementing the theoretical model. This section also defines the baseline airborne radar used to demonstrate the capability of the simulation. Section 4.0 summarizes the findings of this report.

2.0 THEORETICAL MODEL

The theory developed for modeling airborne radars (ABR) is an extension of the one derived in Refs. 1–4 for Space Based Radars (SBR). It is a so–called video simulation which models the signals found in the video section of the radar. The results of Refs. 1–4 do not apply directly to the airborne radar problem. For SBRs, it is

appropriate to neglect second order phase terms but, as will be seen later, they may be significant for ABRs. The SBR model did not simulate pulse compression waveforms. Eclipsing does not normally constitute a problem for SBRs but occurs for ABRs. Finally, the present work allows for a frequency stepped waveform and the use of guard antennas, features not included in the SBR model.

Table I describes the capabilities of the simulation. Although some of these options are not available in the equipment used by the CF, they are included in order to allow for the investigation of more advanced systems.

TABLE I

AIRBORNE RADAR SIMULATOR OPTIONS

CONFIGURATIONS	Pulse Doppler Radar Displaced Phase Center Antenna Multiple Phase Centers Guard Antennas
WAVEFORMS	No Frequency Modulation Linear Frequency Modulation Frequency Hopping Clutter–lock circuitry
MODES OF OPERATION	Air–to–Air Air–to–Ground (Look–Down) Rear Attacks

Table I shows the various Airborne Radar Simulator options. For the four configurations listed in Table I, the location of the radar transmit phase center is in the middle of the antenna. In the conventional Pulse Doppler Radar (PDR) configuration, the locations of the receive and the transmit phase centers coincide. In the Displaced

Phase Center Antenna (DPCA) configuration, there are typically two or three receive phase centers. Their locations are such that the motion of the airborne platform does not degrade clutter cancellation. In the Multiple Phase Centers configuration, the radar uses a large number of receive phase centers. Appropriate weighting of the received signals by the antenna beamformer reduces jamming interference and possibly clutter. In the Guard Antenna configuration, the signal on the main antenna is weighted with the signal from one or more separate guard antennas. This achieves jamming and clutter reduction through antenna sidelobe nulling or blanking.

The waveform is a burst of radio frequency pulses without frequency modulation (NFM) or with linear frequency modulation (LFM) for pulse compression. For the detection of fast moving targets, the usual choice is the NFM waveform with a high pulse repetition frequency (HPRF). The LFM mode normally goes with a low pulse repetition frequency (LPRF) for range unambiguous operation and with a medium pulse repetition frequency (MPRF) for the detection of ground targets (look–down mode). The carrier frequency of the waveform can change from pulse to pulse to improve the performance of the radar against clutter and jamming.

In the following sections, a model for the simulation of ABRs is developed. This model includes computation of the signals for a point target, clutter and the receiver thermal noise. Finally, the average Signal–to–Noise ratio at the output of the radar signal processor is derived. The model allows one to study the average performance of airborne radars without having to use time–consuming Monte Carlo techniques.

2.1 The Geometry

The calculation of the radar signals employs a geocentric frame of reference shown in Fig. 1. The earth is assumed to be circular with a radius equal to r_e. The value of r_e normally equals 6378 km, but can be multiplied by 4/3 or any other appropriate factor to account for the effect of the refraction of the atmosphere. In Fig. 1, T_s, R_i and C represent respectively the locations of the transmit phase center, the i^{th} receive phase center and a point scatterer (target or clutter). The distance between T_s and R_i equals d/2. Let $\vec{r}_s[t]$ and $\vec{r}_c[t]$ be the vectors describing the position of T_s and C, and $\hat{i}$ be a unit vector along the line joining T_s and R_i. It should be noted that throughout this report, square brackets always indicate the functional dependence of a variable on the parameter within the brackets. The radar (both T_s and R_i) and the target are moving at velocities $\vec{v}_s[t]$ and $\vec{v}_c[t]$ respectively. The velocity vector $\vec{v}_s[t]$ includes the contribution from the airspeed, the yaw, the roll and the pitch of the airplane. The velocity of the radar is not necessarily equal to the velocity of the center of mass of the aircraft. This is immaterial in our calculations since we model the radar independently from the aircraft. The time elapsed between the transmission and the reception of the waveform is of the order of 10^{-2}s for a typical ABR. Hence, $\vec{v}_s[t]$ and $\vec{v}_c[t]$ can be considered constant during the measurement and equal to their values at t=0.

Without loss of generality, one can specify that at t=0, T_s rests on the Z axis of the calculation reference frame. At this time, a burst of rectangular RF pulses is transmitted from the radar transmitter. The field sensed by R_i is a collection of delayed replicas of the transmitted waveform, backscattered by the targets within the field of view of the radar. The delay between transmission and reception of the waveform is a non–linear function of time which is the subject of the next sub–section.

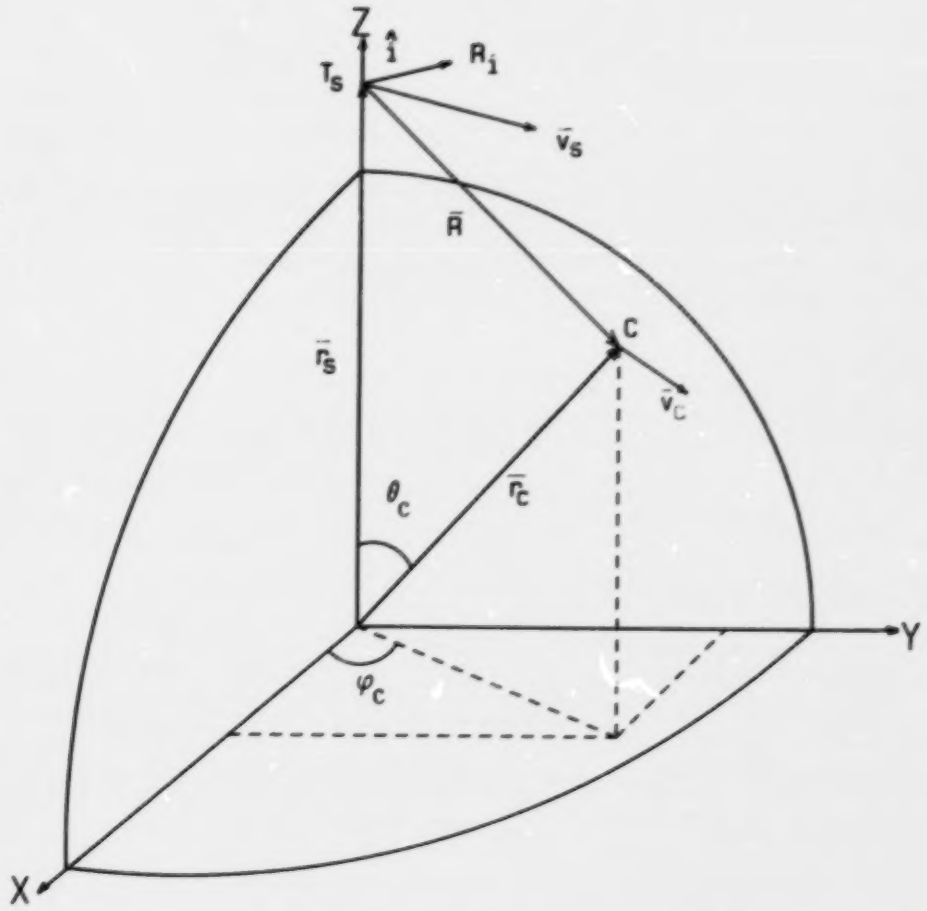

Fig. 1 – Geometry of the problem

2.2 The Propagation Delay

Let t_c be the time at which a given portion of the waveform transmitted at t_0 reaches C and t_i be the time at which the field backscattered by C intercepts R_i. The

propagation delay, Δ_i, is a function of t_0, t_c and t_i and is given by

$$\Delta_i[t_0,t_c,t_i] = (t_c - t_0) + (t_i - t_c) = t_i - t_0 \tag{1}$$

The term $(t_c - t_0)$ can be evaluated by using the following equation:

$$c(t_c - t_0) = |\vec{r}_c[t_c] - \vec{r}_s[t_0]| \tag{2}$$

where c is the speed of light and where | | stands for the norm of the vector. The vectors $\vec{r}_c\,[t_c]$ and $\vec{r}_s\,[t_0]$ in Eq. 2 can be evaluated from the following relations:

$$\vec{r}_c[t_c] = \vec{r}_c[0] + t_c\vec{v}_c[0] \tag{3}$$

and

$$\vec{r}_s[t_0] = \vec{r}_s[0] + t_0\vec{v}_s[0] \tag{4}$$

In order to simplify the notation, we omit the functional dependence on time of the various parameters involved in the calculations when t=0. With this convention and the help of Eqs. 3 and 4, Eq. 2 becomes:

$$c(t_c - t_0) = |\vec{r}_c + t_c\vec{v}_c - \vec{r}_s - t_0\vec{v}_s| \tag{5}$$

Let $\vec{R}(t)$ be the vector joining T_s to C:

$$\vec{R}(t) = \vec{r}_c[t] - \vec{r}_s[t] \tag{6}$$

Expanding Eq. 5 and using Eq. 6, one obtains

$$(t_c - t_0) = \left\{ |\vec{R}|^2 + 2t_c \vec{R}\cdot\vec{v}_c - 2t_0 \vec{R}\cdot\vec{v}_s + |t_c\vec{v}_c - t_0\vec{v}_s|^2 \right\}^{1/2} \tag{7}$$

To further simplify the notation, we represent the norm of a vector by omitting the arrow ($\vec{}$) on top of the corresponding vector.

Then we expand Eq. 7 into a Taylor power series

$$\begin{aligned} c(t_c - t_0) &= R + t_c \hat{R}\cdot\vec{v}_c - t_0 \hat{R}\cdot\vec{v}_s + \frac{|t_c\vec{v}_c - t_0\vec{v}_s|^2}{2R} \\ &\textit{-\frac{1}{8R}\left\{ 2t_c \hat{R}\cdot\vec{v}_c - 2t_0 \hat{R}\cdot\vec{v}_s + \frac{|t_c\vec{v}_c - t_0\vec{v}_s|^2}{R} \right\}^2 + \ldots} \end{aligned} \tag{8}$$

For SBR's, the quadratic and higher order terms of Eq. 8 (in italics) are small compared to the wavelength of the radar. This is because for SBRs, the range to the closest target, R, is hundreds or even thousands of kilometers and λ_c is typically an order of magnitude longer than for ABRs. By using the worst case values given in Table II, it is readily apparent that for ABRs, the second order terms of Eq. 8 can be significant. Neglecting cubic and higher order terms which are negligible, Eq. 8 becomes:

$$\begin{aligned} c(t_c - t_0) = R + t_c \hat{R}\cdot\vec{v}_c - t_0 \hat{R}\cdot\vec{v}_s + \frac{|t_c\vec{v}_c - t_0\vec{v}_s|^2}{2R} \\ -\frac{1}{2R}\left\{ t_c \hat{R}\cdot\vec{v}_c - t_0 \hat{R}\cdot\vec{v}_s \right\}^2 \end{aligned} \tag{9}$$

TABLE II

WORST CASE VALUES FOR ABR CALCULATIONS

Maximum platform velocity (v_s)	Mach 1 (approximately 300 m/s)
Maximum target velocity (v_c)	Mach 1
Maximum radial velocity (V_r)	Mach 2 (approximately 600 m/s)
Maximum normal velocity (V_n)	Mach 1
Target maximum range	100 km
Target minimum range	100 m
Maximum time elapsed (t_0, t_c, t_i)	10^{-2}s

Eq. 9 can be simplified further. The value of $(t_c - t_0)$ is approximately equal to $2R/c$. Hence for small values of R , $(t_c - t_0)$ is small and it can be assume that, for the quadratic terms only, $t_c = t_0$. For large values of R, the approximation breaks down but in this case, the value of the quadratic terms is small due to the R^{-1} coefficient. The error made by using this approximation is of the order of $10^{-3}\lambda_c$. Hence Eq. 9 becomes:

$$c(t_c - t_0) = R + t_c \hat{R}\cdot\vec{v}_c - t_0 \hat{R}\cdot\vec{v}_s + t_c^{\,2}\frac{|\vec{v}_c - \vec{v}_s|^2}{2R} - \frac{t_c^{\,2}}{2R}\left\{\hat{R}\cdot(\vec{v}_c - \vec{v}_s)\right\}^2 \qquad (10)$$

The relative velocity between the radar and the target, $\vec{V}$, is

$$\vec{V} = \vec{v}_c - \vec{v}_s \qquad (11)$$

and the magnitude of the radial relative velocity, $\vec{V}_r$, is

$$V_r = \hat{R} \cdot \vec{V} \tag{12}$$

The magnitude of the normal component of the relative velocity between the radar and the target, $\vec{V}_n$, is:

$$V_n^2 = V^2 - V_r^2 \tag{13}$$

Using Eq. 11–13, the propagation delay from the radar to the target can therefore be written in a more compact form as

$$c(t_c - t_0) = R + t_c \hat{R} \cdot \vec{v}_c - t_0 \hat{R} \cdot \vec{v}_s + \frac{t_c^2}{2R} V_n^2 \tag{14}$$

In Eq. 14, the radial component of the relative velocity between the radar and the target results in a linear phase shift of the signal (Doppler effect). On the other hand, the normal component produces a quadratic phase term (Ref. 5).

The next propagation delay which must be evaluated in Eq. 1 is $c(t_i - t_c)$. This term can be calculated by use of the following relationship:

$$c(t_i - t_c) = |\vec{r}_i[t_i] - \vec{r}_c[t_c]| \tag{15}$$

The vector $\vec{r}_i(t)$ can be written:

$$\vec{r}_i[t] = \vec{r}_s[t] + (d/2)\hat{i} = \vec{r}_s + t_i\vec{v}_s + (d/2)\hat{i} \qquad (16)$$

Following the procedure used to derive Eq. 14 and dropping third and higher order terms, one obtains after some tedious but straightforward manipulations:

$$c(t_i - t_c) = R - t_i\hat{R}\cdot\vec{v}_s + t_c\hat{R}\cdot\vec{v}_c - \frac{d}{2}\hat{R}\cdot\hat{i} - \frac{dt_i}{2R}\vec{V}\cdot\hat{i} + \frac{t_i^2}{2R}V_n^2 + \frac{d^2}{8R} \qquad (17)$$

The total time elapsed from transmission to reception can be found by replacing Eqs. 14 and 17 in Eq. 1. However, in order to simplify the calculations of the radar video signal, it is preferable to express Δ_i in terms of a single time variable, t_i. Hence, from Eq. 14, we can express ct_0 as:

$$ct_0 = -\left\{R + t_c(\hat{R}\cdot\vec{v}_c - c) + \frac{t_c^2}{2R}V_n^2\right\}\left\{1 - \frac{\hat{R}\cdot\vec{v}_s}{c}\right\}^{-1} \qquad (18)$$

Expanding Eq. 18 in a Taylor power series and neglecting again third and higher order terms, it becomes

$$ct_0 = -\left\{R + t_c(V_r - c) + \frac{\vec{R}\cdot\vec{v}_s}{c} + \frac{t_c^2}{2R}V_n^2\right\} \qquad (19)$$

Using Eq. 17, we can compute t_c as a function of t_i:

$$ct_c = -\left\{R - \frac{d}{2}(\hat{R}\cdot\hat{i}) + \frac{d^2}{8R} - t_i\left[c - V_r + \frac{d}{2R}\vec{V}\cdot\hat{i}\right] + \frac{t_i^2}{2R}V_n^2 - \frac{\vec{R}\cdot\vec{v}_c}{c}\right\} \qquad (20)$$

Using Eqs. 19 and 20, one can finally compute Δ_i from Eq. 1. Neglecting again the third and higher order terms, the result for the overall propagation delay is

$$\Delta_i[t_i] = \frac{2R}{c} - \frac{2RV_r}{c^2} - d\frac{\hat{R}\cdot\hat{i}}{2c} + \frac{d^2}{8Rc} + \frac{t_i\left[2V_r - (d/2R)\vec{V}\cdot\hat{i}\right]}{c} + \frac{V_n^2 t_i^2}{Rc} \qquad (21)$$

Eq. 21 is identical to the equations obtained in Refs. 1, 4, except for the terms in italics which are second order effects neglected for SBRs.

Although the calculations leading to Eq. 21 are rather tedious, the equation conveys a clear physical meaning. The term 2R/c is the gross delay time required for the RF pulses to travel back and forth to the target. The term $2RV_r/c^2$ accounts for the delay resulting from the distance travelled by the target during the gross delay 2R/c. The term $-(d/2c)\hat{R}\cdot\hat{i}$ is the time required to reach the i^{th} phase center. This can be shown by referring to Fig. 2, where $\overline{AR}_i$ is the distance between points A and R_i:

$$\begin{aligned}\overline{AR}_i &= (d/2)\cos[\theta] \\ &= -(d/2)\cos[(\pi/2)+\theta] \\ &= -(d/2)\,\hat{R}\cdot\hat{i}\end{aligned} \qquad (22)$$

Therefore $-(d/2c)\hat{R}\cdot\hat{i}$ is the time to reach the i^{th} phase centre. The term $d^2/8Rc$ is a rather small second order effect ($d^2/8R \simeq 4\times10^{-2}\ \lambda_c$). The term $2t_iV_r$ is the Doppler shift experienced by the RF radiation received by R_i. The term $-t_i(d/2R)\vec{V}\cdot\hat{i}/c$ is a second order effect arising because the radial velocity of the target and hence its Doppler shift is a function of the location of R_i. This can be explained by referring to Fig. 2. Let $\vec{V}_r^i$ be the radial velocity of point C relative to R_i and $\vec{R}_{ic}$ be a line joining R_i and C. We thus have:

$$\begin{aligned}\vec{V}_r^i &= (\vec{v}_c-\vec{v}_s)\cdot\hat{R}_{ic}\\ &= \vec{V}\cdot\frac{\vec{R}_{ic}}{R_{ic}}\cong\frac{\vec{V}}{R}\cdot\{\vec{R}-(d/2)\hat{i}\}\\ &= \vec{V}_r-(d/2R)\,\vec{V}\cdot\hat{i}\end{aligned}\qquad(23)$$

Finally, the term $V_n^2t_i^2/Rc$ is a second order phase term caused by the component of the motion of the target which is normal to $\vec{V}$.

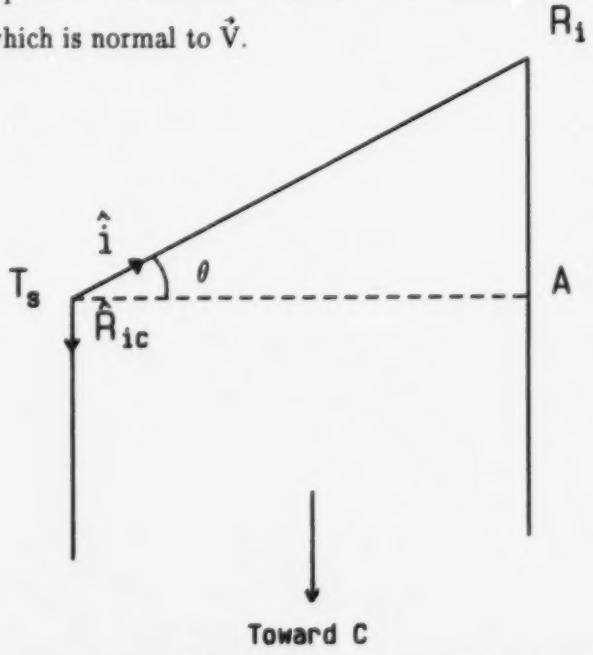

Fig. 2 – Location of the phase centers and the target

To facilitate the derivation and the interpretation of the expressions for the radar signals, $\Delta_i[t_i]$ is rewritten by grouping together the various powers of t_i and dropping the subscript i of t_i:

$$\Delta_i[t] = \delta_0 + \delta_1 t + \delta_2 t^2 \tag{24}$$

where

$$\delta_0 = \frac{2R}{c} - \frac{2RV_r}{c^2} - d\frac{\hat{R}\cdot\hat{i}}{2c} + \frac{d^2}{8Rc} \tag{25}$$

$$\delta_1 = \frac{2V_r - (d/2R)\vec{V}\cdot\hat{i}}{c} \tag{26}$$

$$\delta_2 = \frac{V_n^2}{Rc} \tag{27}$$

The radar signal received from a target is a replica of the transmitted signal, delayed by the propagation time. The modeling of the transmitted signal is the subject of the following section.

2.3 The Transmitted Radar Signal

The radar transmits a waveform described by

$$u[t] = K_t\, g_t \exp[j\omega_c t] \cdot \nu[t] \tag{28}$$

where ω_c and $\nu[t]$ are respectively the carrier frequency and the complex modulation

function of the radar waveform, K_t is a scaling factor accounting for the power level transmitted and g_t is the complex directivity of the transmit phase center. The constant K_t is given by:

$$K_t = \sqrt{P_k/4\pi} \tag{29}$$

where P_k is the peak transmitted power.

In this work, $\nu[t]$ is a train of N_p rectangular pulses of duration τ_p, with provision for frequency hopping from pulse to pulse:

$$\nu[t] = \sum_{k=0}^{N_p-1} \Pi\left[\frac{t-k\tau_r}{\tau_p}\right] \cdot \mu[t-k\tau_r] \cdot \exp[j\omega_k t] \tag{30}$$

where $\mu[t]$ is the single pulse modulation function, ω_k is the angular frequency increment for the k^{th} pulse and τ_r is the Pulse Repetition Interval (PRI). The definition of the rectangle function, $\Pi[t]$, is

$$\begin{aligned} \Pi[t] &= 1 \quad \text{for } t \in [0,1] \\ &= 0 \quad \text{elsewhere} \end{aligned} \tag{31}$$

If the waveform does not have frequency hopping , ω_k is simply set equal to zero in Eq. 30.

In this work, we allow for two single pulse modulation functions. The first one, μ_{NFM}, describes a waveform without frequency modulation. The second one, μ_{LFM}, describes a waveform with linear frequency modulation for pulse compression. The equations for these single pulse modulation functions are:

$$\mu_{NFM}[t] = 1 \tag{32}$$

and

$$\mu_{LFM}[t] = \exp[j\pi bt^2] \quad 0 \leq t \leq \tau_p \tag{33}$$

where b is the linear frequency sweep rate related to the frequency sweep, B, by:

$$b = \pm B/\tau_p \tag{34}$$

The sign ± in front of B indicates that the frequency of the RF pulse can either be up–shifted or down–shifted, according to the sign chosen. Since B is approximately equal to the inverse of the compressed radar pulse width, τ_c, we have that

$$|b| \approx 1/\tau_p\tau_c \tag{35}$$

2.4 The Signal from a Point Source

For clarity and completeness, we describe the signal at various points along the radar receiver shown in Fig. 3. Let $y_i^r[t]$ be the signal at the location of the ith phase

center. This signal is a delayed replica of the transmitted signal backscattered by a point target, so that:

$$y_i^r[t] = K_r \, g_i^a \, \rho \, u\left[t - \Delta_i[t]\right] \tag{36}$$

where g_i^a is the directivity of the ith phase center, and ρ is the complex reflectivity of the point target. The constant K_r accounts for the system losses, L_s, and the geometric propagation losses and is given by:

$$K_r = \left[\frac{\lambda^2}{(4\pi)^2 R^4 L_s}\right]^{1/2} \tag{37}$$

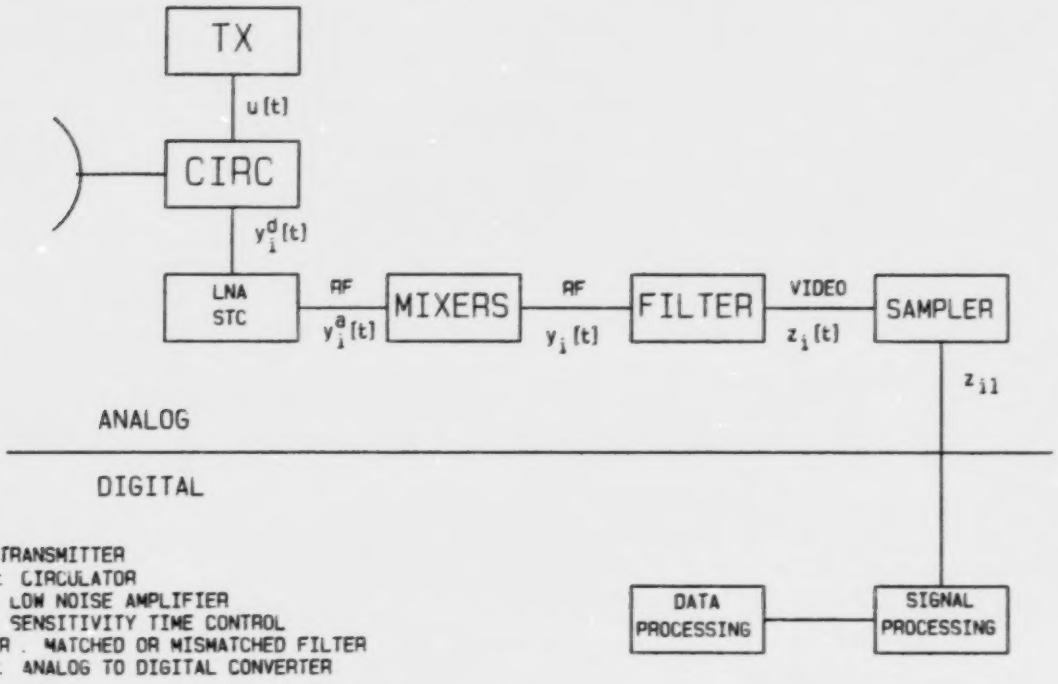

Fig. 3 – Radar system block diagram

Normally the receiver does not operate when the transmitter transmits the waveform. Therefore, in order to obtain $y_i^d[t]$, the signal actually sensed by the ith phase center, one has to multiply $y_i^r[t]$ by an eclipsing function, E[t]:

$$y_i^d[t] = y_i^r[t] \cdot E[t] \tag{38}$$

The form of E[t] can be determined by inspection, from Fig. 4.

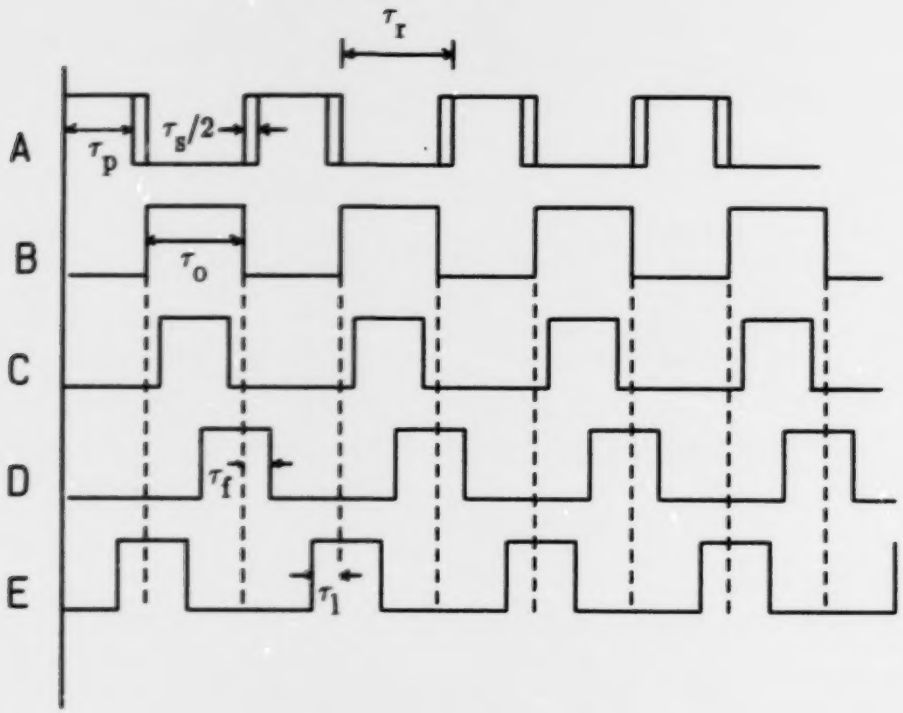

Fig. 4 – Diagram showing the transmitted and the received waveforms: 4a shows the transmitted waveform and the the receiver switching time; 4b is the eclipsing function; 4c is the waveform without eclipsing; 4d and 4e show eclipsing of respectively the end and the front of the radar pulses.

Fig. 4a shows the transmitted waveform. We assume that the radar transmits the RF pulses on a continuous basis rather than transmitting N_p pulses and turning off for some time before repeating the process over again. As shown in Fig. 4a, the receiver is inoperative for a time equal to $\tau_s/2$. This is the time during which the system switches from the transmit to the receive state. The time during which the receiver is functional is shown in Fig. 4b. This is the eclipsing function, E[t]. It is a series of rectangle functions of duration τ_o given by

$$E[t] = \sum_{k=0}^{\infty} \Pi\left[\frac{t - k\tau_r - \tau_p - \tau_s/2}{\tau_o}\right] \tag{39}$$

where τ_o is

$$\tau_o = \tau_r - \tau_p - \tau_s \tag{40}$$

Fig. 4c shows the received pulse train for the case where there is no eclipsing. Fig. 4d and 4e show the received pulse train for the cases where the front and the end of the pulses are eclipsed. Thus, the eclipsed signal is a train of pulses with each pulse being equal to or shorter than τ_p. Let τ_1 be the duration of the eclipsed pulses and let τ_f be the portion of the leading edge of the pulse which may have been eclipsed. We can thus write $y_i^d[t]$ as:

$$y_i^d[t] = K\, g_t\, g_i^a\, \rho \exp\left[j\omega_c(t-\Delta_i[t])\right] \times$$

$$\sum_{k=0}^{N_p-1} \Pi\left[\frac{t-k\tau_r-\Delta_i[t]-\tau_f}{\tau_l}\right] \mu\left[t-k\tau_r-\Delta_i[t]\right] \exp\left[j\omega_k(t-\Delta_i[t])\right] \qquad (41)$$

where $K=K_tK_r$.

Let k' be the number of PRI's elapsed before the first pulse from the target reaches the receiver. The parameter k' is thus largest integer such that

$$k' \leq (\frac{2R}{c})/\tau_r \qquad (42)$$

To calculate the values of τ_f and τ_l, we must consider four possibilities.

1) **No eclipsing.**

This occurs when

$$k'\tau_r+\tau_p+\tau_s/2 \leq 2R/c \leq (k'+1)\tau_r-\tau_p-\tau_s/2 \qquad (43)$$

and in this case

$$\tau_f = 0 \qquad (44)$$

$$\tau_l = \tau_p \qquad (45)$$

2) **The leading edge of the pulse is eclipsed.**

This occurs when

$$2R/c < k'\tau_r+\tau_p+\tau_s/2 \tag{46}$$

and in this case

$$\tau_f = k'\tau_r+\tau_p+\tau_s/2-2R/c \tag{47}$$

$$\tau_l = \tau_p - \tau_f \tag{48}$$

3) **The trailing edge of the RF pulse is eclipsed.**

This occurs when

$$2R/c > (k'+1)\tau_r-\tau_p-\tau_s/2 \tag{49}$$

and in this case

$$\tau_f = 0 \tag{50}$$

$$\tau_l = (k'+1)\tau_r-2R/c-\tau_s/2 \tag{51}$$

4) **The whole RF pulse is eclipsed.**

This occurs when

$$k'\tau_r-\tau_s/2 \leq 2R/c \leq k'\tau_r+\tau_s/2 \tag{52}$$

and in this case, no energy is detected by the radar.

Once the signal is received from the target, it is amplified and converted to baseband. The video signal is thus:

$$y_i[t] = g^{amp}\, y_i^d[t] \exp\left[-j\omega_c t\right] \tag{53}$$

where g^{amp} is the gain in the amplification chain including Sensitivity Time Control (STC).

To a very good approximation, one can assume that for the envelope of the received signal, $\Delta_i[t]$ is equal to the gross time delay, 2R/c, so that, using Eq. 41 for $y_i^d[t]$, the final expression for the video signal is

$$y_i[t] = g_i\, \rho \exp\left[-j\omega_c \Delta_i[t]\right] \times$$

$$\sum_{k=0}^{N_p-1} \Pi\left[\frac{t-2R/c-k\tau_r-\tau_f}{\tau_l}\right] \mu\left[t-k\tau_r-\Delta_i[t]\right] \exp\left[j\omega_k(t-\Delta_i[t])\right] . \tag{54}$$

where

$$g_i = K_t\, K_r\, g_i^a\, g^{amp} \tag{55}$$

In the next sub section, Eq. 54 is evaluated separately for the NFM and the LFM waveforms.

2.4.1 The NFM Waveform

As shown in Fig. 3, the first operation performed on the NFM signal is match filtering. In general, the impulse response of a filter matched to a waveform f[t] is given by:

$$h[t] = K_m f^*[-t] \tag{56}$$

where K_m is a normalization constant. In this work, the received signal is matched to a single rectangular pulse of the transmitted burst. However, the mathematical expression for the matched filter may or may not include the frequency steps ω_k. To account for these two possibilities, the center frequency of the matched filter is shifted by ω_k' where $\omega_k'=0$ for clutter suppression and $\omega_k'=\omega_k$ for ECCM.

To simulate the operation of a clutter–lock circuit (Ref. 6), the transfer function of the matched filter is translated by the doppler frequency ω_d. In this manner, its center frequency corresponds to the Doppler shifted frequency of main beam clutter. The impulse response of the matched filter for the NFM waveform is thus:

$$h_m[t] = K_{NFM}\, \Pi\left[-t/\tau_p\right] \exp\left[j\omega_{dk}t\right] \tag{57}$$

where

$$\omega_{dk} = \omega_d + \omega_k' \tag{58}$$

and where $K_{NFM} = K_M$ for the NFM waveform. Equation (57) implies that the width

of the range gates is equal to τ_p. In practical systems, this is not always the case. To account for this possibility, the impulse response of the NFM filter is written as

$$h_{NFM}[t] = K_{NFM}\,\Pi\left[-t/\tau_g\right]\exp\left[j\omega_{dk}t\right] \tag{59}$$

where τ_g is the width of the range gates ($\tau_p \le \tau_g \le \tau_o$).

Requiring that the transfer function has unit amplitude at $\omega = \omega_d$, we find that K_{NFM} is

$$K_{NFM} = 1/\tau_g \tag{60}$$

The matched filtered signal, $z_i[t]$, is obtained by convolving Eq. 54 with Eq. 59 to give:

$$z_i[t] = K_{NFM}\,g_i\,\rho \int_{-\infty}^{\infty} \exp\left[-j\omega_c\Delta_i[\eta]\right] \times$$

$$\sum_{k=0}^{N_p-1} \Pi\left[\frac{\eta-2R/c-k\tau_r-\tau_f}{\tau_l}\right]\exp\left[j\omega_k(\eta-\Delta_i[\eta])\right] \times$$

$$\Pi\left[-\frac{(t-\eta)}{\tau_g}\right]\exp\left[j\omega_{dk}(t-\eta)\right]\,d\eta \tag{61}$$

Defining

$$\eta' = \eta - t \tag{62}$$

and

$$\alpha[t] = -t+2R/c+k\tau_r+\tau_f \tag{63}$$

we obtain

$$z_i[t] = K_{NFM}\, g_i\, \rho \exp\left[j\omega_k t\right] \times$$

$$\sum_{k=0}^{N_p-1} \int_{-\infty}^{\infty} \exp\left[-j(\omega_c+\omega_k)\Delta_i[\eta'+t] + j(\omega_k-\omega_{dk})\eta'\right] \times$$

$$\Pi\left[\frac{\eta'-\alpha[t]}{\tau_1}\right] \Pi\left[\frac{\eta'}{\tau_g}\right] d\eta' \tag{64}$$

As shown in Fig. 5, the product of the two rectangle functions in Eq. 64 differs from zero only over an interval defined by

$$-\tau_1 \leq \alpha[t] \leq \tau_g \tag{65}$$

Inequality 65 can be rewritten as:

$$t-2R/c-\tau_p \leq k\tau_r \leq t-2R/c-\tau_f+\tau_g \tag{66}$$

Since $\tau_g+\tau_p \leq \tau_r$, Eq. 66 shows that for any given values of t and R, there is only one value of k, $\tilde{k}$, satisfying the inequality. Physically, this means that only the $\tilde{k}^{th}$ pulse in

the transmitted burst contributes to the signal received at time t from a point target at a distance R away from the radar.

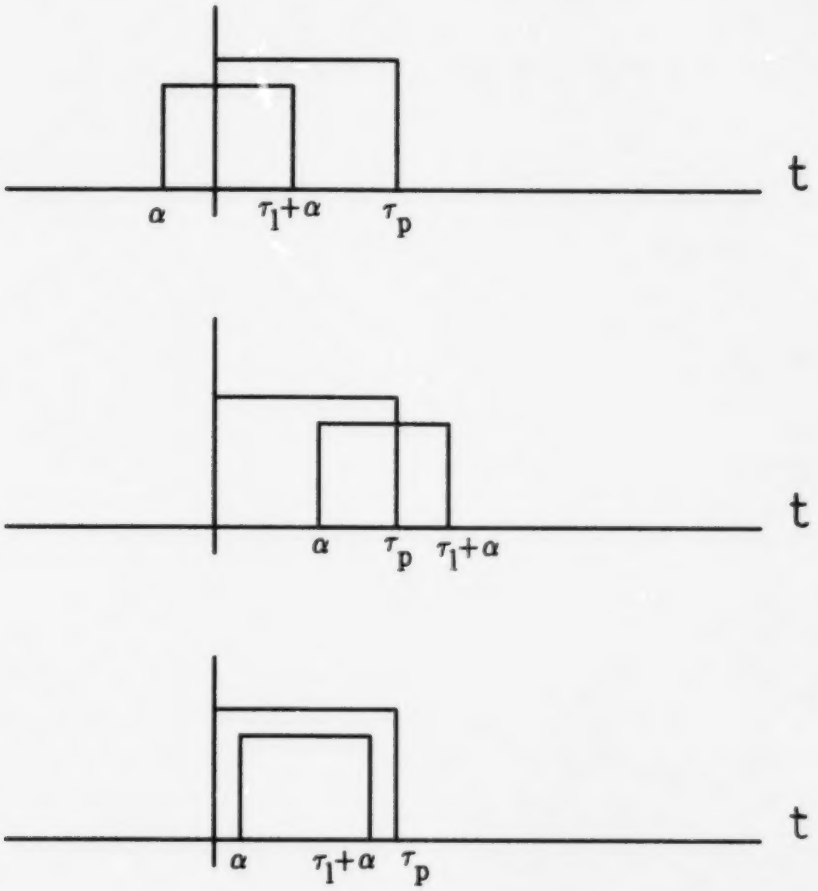

Fig. 5 – Integration limits for the NFM waveform

Referring to Fig. 5, the limits of integration in Eq. 64 extend from η'_{min} to η'_{max} where

$$\eta'_{min}[t] = \Big[\alpha[t] + |\alpha[t]|\Big]/2 \tag{67}$$

and

$$\eta'_{max}[t] = \tau + \Big[\alpha[t] - |\alpha[t]|\Big]/2 \tag{68}$$

In equation 67 and 68, the value of τ is

$$\tau = \tau_g H\Big[\alpha[t]\Big] + \tau_1 H\Big[-\alpha[t]\Big] \quad \text{for} \quad \alpha[t]<0 \text{ or } \alpha[t]\geq 0 \wedge \tau_1+\alpha[t]\geq\tau_p$$

or

$$\tau = \tau_1+\alpha[t] \qquad \text{otherwise} \tag{69}$$

Where H[t] is the Heaviside step function given by:

$$\begin{aligned} H[t] &= 1 \qquad \text{for } t \geq 0 \\ &= 0 \qquad \text{elsewhere} \end{aligned} \tag{70}$$

Hence, making use of Eq. 67 – 70 and replacing $\Delta_i[t]$ by its value Eq. 24–27, Eq. 64 becomes

$$z_i[t] = K_{NFM} g_i \rho \exp\Big[j\omega_{\tilde{k}} t\Big] \cdot \int_{\eta'_{min}}^{\eta'_{max}} \exp\Big[-j\Omega_{c\tilde{k}}\Big[\delta_0+\delta_1(\eta'+t)+\delta_2(\eta'+t)^2\Big] + j\Omega_{d\tilde{k}}\eta'\Big]\, d\eta' \tag{71}$$

if a value of $\tilde{k}$ in the interval $[0,N_p-1]$ can be found. Otherwise, Eq. 64 is equal to zero.

In Eq. 71, Ω_{ck} and Ω_{dk} are respectively

$$\Omega_{ck} = \omega_k + \omega_c \tag{72}$$

and

$$\Omega_{dk} = \omega_k - \omega_{dk} \tag{73}$$

Since the values of η'_{min} and η'_{max} do not exceed 10^{-4}s for typical ABRs and since δ_2 is small, the terms $\delta_2 \eta'^2$ and $\delta_2 \eta' t$ are negligible. Extracting the terms independent of η' from the integral we obtain after performing the integration

$$z_i[t] = K_{NFM} \frac{2g_i \rho}{\Omega_{\tilde{k}}} \exp\left[j\left\{\omega_{\tilde{k}} t - \Omega_{c\tilde{k}} \Delta_i[t]\right\}\right] \exp\left[\frac{-j\Omega_{\tilde{k}} \ (\tau + \tilde{\alpha}[t])}{2}\right] \times \sin\left[\frac{\Omega_{\tilde{k}} \ (\tau - |\tilde{\alpha}[t]|)}{2}\right] \tag{74}$$

where

$$\Omega_k = \Omega_{ck}\delta_1 - \Omega_{dk} \tag{75}$$

The tilda symbol in Eq. 74 is reminder that the corresponding parameters depend on a unique value of $k=\tilde{k}$.

To simplify the notation for the later calculations of the clutter covariance matrix in Sect. 2.6, we extract all the terms independent of ρ in the expression of $z_i[t]$:

$$z_i[t] = \rho \, \bar{z}_i[t] \tag{76}$$

where

$$\tilde{z}_i[t] = K_{NFM} \frac{2g_i}{\Omega_{\tilde{k}}} \exp\left[j\left\{\omega_{\tilde{k}} t - \Omega_{c\tilde{k}} \Delta_i[t]\right\}\right] \exp\left[\frac{-j\Omega_{\tilde{k}} \ (\tau+\tilde{\alpha}[t])}{2}\right] \times \sin\left[\frac{\Omega_{\tilde{k}} \ (\tau-|\tilde{\alpha}[t]|)}{2}\right] \tag{77}$$

In modern radar receivers, an analog to digital converter (ADC) samples the signal for input to the digital signal processor. Using Eq. 74, one obtains the l^{th} sample of the signal for the range gate at a distance R_g from the radar by letting t equal

$$t = \frac{2R_g}{c} + l\tau_r \tag{78}$$

In the last equation, l is an element of the interval $[0,N_p-1]$.

2.4.2 The LFM Waveform

With an LFM waveform, it is no longer practical to implement a matched filter to process the signal. This is because the transfer function of the matched filter contains ripples which are difficult to implement in practice. This applies especially when the compression ratio is smaller than about twenty (Ref. 7,8). Moreover, the compressed pulses exhibit large sidelobes which must be weighted down to reduce the range sidelobes. It is thus common practice to implement a mismatched filtered (MMF) with LFM waveforms. We thus follow Ref. 7 and model a MMF consisting of compressing the received signal and weighting it in the frequency domain. The transfer function of

the compressor is

$$H_c[\omega] = \exp\left[\frac{j(\omega - \omega_{dk})^2}{4\pi b}\right] \tag{79}$$

As for the NFM case, the center frequency of the filter is shifted by ω_{dk}.

One can easily verify that $H_c[\omega]$ is a compressor by using the group delay concept. The group delay of a filter, τ_d, relates to the velocity at which information or energy flows in a system. It is given by (Ref. 8)

$$\tau_d = -\frac{d}{d\omega}\left[\theta[\omega]\right] \tag{80}$$

where $\theta[\omega]$ is the phase of the transfer function of the filter. Using Eq. 79, the group delay for the compressor is:

$$\tau_d = -\frac{(\omega - \omega_{dk})}{2\pi b} \tag{81}$$

Putting ω_{dk}=0 to simplify the interpretation, this equation shows that the group delay is proportional to the angular frequency of the waveform. Hence, on transmit, the frequency of the waveform is linearly increased at a rate b. On receive, the compressor decreases it at the same rate.

For the sake of simplicity, we use an exponential weighting of the frequency spectrum of the waveform to achieve range sidelobe reduction (Refs. 9,10). Although it

might not be the preferred weighting function from a practical point of view, it performs like the more usual weighting schemes. The weighting operation can be represented by

$$H_p(\omega) = \exp\left[-\frac{q\ (\omega - \omega_{dk})^2}{4\pi}\right] \tag{82}$$

where q is the weighting coefficient. It is adjusted to achieve an attenuation of A_{dB} decibels at the edges of a frequency window extending B Hz on either side of the signal center frequency. One can easily show that q is:

$$q = 0.147\ A_{dB} / B^2 \tag{83}$$

The overall impulse response of the MMF is obtained by computing the Fourier transform of the product of Eq. 79 and Eq. 82. Using the work of Prudnikov et al. (Ref. 11) the result is

$$h_{LFM}[t] = K_{LFM} \exp\left[j\omega_{dk}t - \frac{\pi b(j+bq)_t^2}{q^2b^2+1}\right] \tag{84}$$

where

$$K_{LFM} = \sqrt{\frac{jb + qb^2}{b^2q^2 + 1}} \tag{85}$$

Eq. 84 shows that the impulse response of the MMF is centered on t=0 rather than on $\tau_g/2$ for the NFM case. Hence, for the LFM calculations alone, it is convenient to

redefine the rectangle function in the following manner:

$$\begin{aligned} \Pi[t] &= 1 \qquad \text{for } -1/2 \le t \le 1/2 \\ &= 0 \qquad \text{elsewhere} \end{aligned} \tag{86}$$

In this manner, the maximum output of the filter occurs when the range to the target, R, equals R_g, as is the case for the NFM waveform.

Following the procedure used for the NFM, the signal at the output of the MMF is the convolution of $y_i[t]$ with $h[t]$:

$$z_i[t] = K_{LFM}\, g_i\, \rho \int_{-\infty}^{\infty} \exp\left[-j\omega_c \Delta_i[\eta]\right] \times$$
$$\sum_{k=0}^{N_p-1} \Pi\left[\frac{\eta - 2R/c - k\tau_r - \tau_f}{\tau_l}\right] \exp\left[j\pi b\left[\eta - k\tau_r - \Delta_i[\eta]\right]^2\right] \exp\left[j\omega_k(\eta - \Delta_i[\eta])\right] \times$$
$$\exp\left[j\omega_{dk}(t-\eta) - \frac{\pi b(j+bq)}{q^2b^2+1}(t-\eta)^2\right] d\eta \tag{87}$$

Defining

$$\eta' = \eta - 2R/c - k\tau_r - \tau_f \tag{88}$$

and

$$\beta_k = 2R/c + k\tau_r + \tau_f \tag{89}$$

and using Eq. 63, Eq. 87 becomes

$$z_i[t] = K_{LFM}\, g_i\, \rho \exp\left[-j\omega_{dk}\alpha[t]\right] \times$$

$$\sum_{k=0}^{N_p-1} \exp\left[j\omega_k\beta_k\right] \int_{-\tau_1/2}^{\tau_1/2} \exp\left[-j\Omega_{ck}\Delta_i[\eta'+\beta_k]\right] \exp\left[+j\Omega_{dk}\eta'\right] \times$$

$$\exp\left[j\pi b\left[\eta'+2R/c+\tau_f-\Delta_i\left[\eta'+\beta_k\right]\right]^2\right] \exp\left[-\frac{\pi b(j+bq)}{q^2b^2+1}\left[\eta'+\alpha[t]\right]^2\right] d\eta' \qquad (90)$$

In this equation, the complex exponentials are weighted by a series of Gaussian functions (the second term of the second exponential function):

$$\exp\left[-\frac{\pi q b^2}{q^2b^2+1}\left[\eta'-t+2R/c+k\tau_r+\tau_f\right]^2\right] \qquad (91)$$

The first of these Gaussian functions (k=0) is centered at

$$\eta' = t-2R/c-\tau_f \qquad (92)$$

and the others are τ_r apart around η'. The width of the Gaussian functions between the point $\eta'=0$ and the e^{-1} point, $\aleph$, is by

$$\aleph = \left[\frac{q^2b^2+1}{\pi q b^2}\right]^{1/2} \qquad (93)$$

The parameter $\aleph$ can be expressed in terms of τ_c and τ_p for more clarity. Since q is proportional to τ_c^2 (Eq. 83) and

$$b \propto \frac{1}{\tau_p \tau_c}, \tag{94}$$

we find that

$$\aleph \propto \tau_p \tag{95}$$

since t_p is normally at least ten times greater than t_c.

It is interesting to note that the width of $h_{LFM}[t]$ is proportional to τ_p although the width of $h_p[t]$ is proportional to τ_c. The width of $h_{LFM}[t]$ has to be proportional to τ_p. Otherwise, only a small fraction of the energy returned by the target would be processed by the receiver. This would result in a low the signal to noise ratio.

The interval of integration in Eq. 90 extends only over $[-\tau_1/2,\tau_1/2]$. It is thus likely that one of the Gaussian functions contributes significantly more than the others to the integral. This can be confirmed with the help of the Error function (Ref. 12). The first case of interest is when one of the Gaussian overlaps the interval of integration. Assuming a worst case duty cycle of 20% and no eclipsing, the power contribution of the Gaussian centered on the interval of integration is more than 100 dB larger than the contribution from the adjacent Gaussians. The second case of interest is when the Gaussian functions are symmetrically located on either side of the interval of integration. Their power contribution to the integral is approximately 47 dB lower than that of the Gaussians centered on the interval of integration. These numbers show that,

like for the NFM case, it is sufficient to consider the contribution of only one Gaussian to the integral of Eq. 90. This is the Gaussian which is located the closest to the center of the integration interval. The index of this Gaussian, $\tilde{k}$, is the integer element of $[0,N_p-1]$ which minimizes the expression $t-2R/c-\tilde{k}\tau_r-\tau_f$.

Expanding the value of $\Delta_i[t]$ and assuming that only the $\tilde{k}^{th}$ pulse contributes to the integral, Eq. 90 becomes

$$z_i[t] = K_{LFM}\, g_i\, \rho \exp\left[-j\omega_{d\tilde{k}}\tilde{\alpha}[t]\right] \exp\left[j\omega_{\tilde{k}}\beta_{\tilde{k}}\right] \times$$

$$\int_{-\tau_1/2}^{\tau_1/2} \exp\left[-j\Omega_{c\tilde{k}}\left\{\delta_0+\delta_1\left[\eta'+\beta_{\tilde{k}}\right]+\delta_2\left[\eta'+\beta_{\tilde{k}}\right]^2\right\}\right] \exp\left[+j\Omega_{d\tilde{k}}\eta'\right] \times$$

$$\exp\left[j\pi b\left\{\eta'+2R/c+\tau_f-\delta_0-\delta_1\left[\eta'+\beta_{\tilde{k}}\right]-\delta_2\left[\eta'+\beta_{\tilde{k}}\right]^2\right\}^2\right] \times$$

$$\exp\left[-\frac{\pi b(j+bq)}{q^2b^2+1}\left[\eta'+\alpha[t]\right]^2\right] d\eta' \qquad (96)$$

Using Table I, one finds that many terms in Eq. 96 are negligible over the interval of integration. The last equation thus reduces to

$$z_i[t] = K_{LFM}\, g_i\, \rho \exp\left[-j\omega_{d\tilde{k}}\tilde{\alpha}[t]\right] \exp\left[j\omega_{\tilde{k}}\beta_{\tilde{k}}\right]$$

$$\exp\left[-j\Omega_{c\tilde{k}}\Delta_i\left[\beta_{\tilde{k}}\right]-\frac{\pi b(j+bq)}{q^2b^2+1}\tilde{\alpha}^2[t]+j\pi b\left[\tau_f-\beta_{\tilde{k}}\delta_1\right]^2\right]$$

$$\int_{-\tau_1/2}^{\tau_1/2} \exp\left[-j\left\{\Omega_{c\tilde{k}}\delta_1 - \Omega_{d\tilde{k}} - 2\pi b\left[\tau_f - \beta_{\tilde{k}}\delta_1\right] + j\frac{\pi b(j+bq)}{q^2b^2+1}2\alpha[t]\right\}\eta'\right] \times$$

$$\exp\left[\left\{j\pi b - \frac{\pi b(j+bq)}{q^2b^2+1}\right\}\eta'^2\right] d\eta' \qquad (97)$$

Let

$$X^2 = -j\pi b + \frac{\pi b(j+bq)}{q^2b^2+1} \qquad (98)$$

and

$$Y = -(1/2X^2)\left\{j\Omega_{c\tilde{k}}\delta_1 - j\Omega_{d\tilde{k}} - j2\pi b\left[\tau_f - \beta_{\tilde{k}}\delta_1\right] + \frac{\pi b(j+bq)}{q^2b^2+1}2\alpha[t]\right\} \qquad (99)$$

By completing the squares we obtain after some manipulations

$$z_i[t] = \frac{K_{LFM}}{X} g_i\rho \exp\left[-j\omega_{dk}\tilde{\alpha}[t]\right] \exp\left[j\omega_{\tilde{k}}\beta_{\tilde{k}}\right] \times$$

$$\exp\left[-j\Omega_{c\tilde{k}}\Delta_i\left[\beta_{\tilde{k}}\right] - \frac{\pi\ b(j+bq)}{q^2b^2+1}\tilde{\alpha}^2[t] + j\pi b\left[\tau_f - \beta_{\tilde{k}}\delta_1\right]^2 + X^2Y^2\right] \times$$

$$\sqrt{\pi}/2\left\{\mathrm{Erfc}\left[X\left[Y-\tau_1/2\right]\right] - \mathrm{Erfc}\left[X\left[Y+\tau_1/2\right]\right]\right\} \qquad (100)$$

where Erf[x] is the complementary Error Function defined as

$$\mathrm{Erfc}[x] = 1 - \mathrm{Erf}[x] \qquad (101)$$

In order to simplify the notation for the calculation of the clutter covariance matrix in Sect. 2.6, the terms independent of ρ are extracted out of the expression for $z_i[t]$:

$$z_i[t] = \rho\, \bar{z}_i[t] \tag{102}$$

where

$$\bar{z}_i[t] = K_{LFM} \frac{g_i}{X} \exp\left[-j\omega_{dk}\tilde{\alpha}[t]\right] \exp\left[j\omega_{\tilde{k}}\beta_{\tilde{k}}\right] \cdot$$

$$\exp\left[-j\Omega_{c\tilde{k}}\Delta_i\left[\beta_{\tilde{k}}\right] - \frac{\pi b(j + bq)}{q^2 b^2 + 1}\tilde{\alpha}^2[t] + j\pi b\left[\tau_f - \beta_{\tilde{k}}\delta_1\right]^2 + X^2Y^2\right] \cdot$$

$$\sqrt{\pi}/2\left\{\mathrm{Erfc}\left[X\left[Y-\tau_1/2\right]\right] - \mathrm{Erfc}\left[X\left[Y+\tau_1/2\right]\right]\right\} \tag{103}$$

Eqs. 76 and 102 describe the signal received from a point target for respectively the NFM and LFM waveforms. They can also be used to obtain the signal from a distributed target. Our interest in this work is primarily ground clutter against which point targets have to compete for detection. This is the subject of the next two sections. The following calculations can easily be extended to volumetric clutter (rain or chaff). A similar procedure would also apply to compute the signal from complex targets that can be resolved by the radar.

2.5 The Signal from a Distributed Target

The signal from a distributed target is the sum of the signals from a collection of contiguous elemental scatterers spanning the target. In the case of the clutter, the reflectivity of an elemental clutter patch of area dA_c is

$$\rho_c = \rho_c^{\circ}[\gamma_c]\, dA_c \tag{104}$$

In Eq.104, $\rho_c^{\circ}[\gamma_c]$ is the clutter reflectivity per unit area and is a function of the grazing angle, γ_c. Ref. 1 shows that the area of a clutter patch on a spherical surface (the earth) is

$$dA_c = \frac{r_e}{r_s} R_c\, dR_c\, d\varphi_c \tag{105}$$

where the subscript c refers to a clutter patch. The signal from an elemental clutter patch, dc_{il}, is given by Eqs. 76 and 77 for the NFM case or by Eqs. 102 and 103 for the LFM case. For clutter, ρ_c replaces ρ and the range and the velocity parameters are those of the clutter element under consideration.

The total clutter return is the integral of the elemental contributions over the terrain within the footprint of the antenna:

$$c_i[t] = \int_{R_c} \int_{\varphi_c} dc_i[t] \tag{106}$$

The limits of integration extend at most over the following interval:

$$\varphi_c \in [0,2\pi] \tag{107}$$

and

$$R_c \in \left[h , (r_s^2 - r_e^2)^{1/2} \right] \tag{108}$$

where h is the altitude of the aircraft and $(r_s^2 - r_e^2)^{1/2}$ is the range to a point on the Earth's horizon as seen from the radar. Clearly, because of the weighting effect of the radar antenna gain pattern, only a small fraction of the clutter patches contribute significantly to the clutter return.

2.6 The Clutter Covariance Matrix

As discussed in Refs. 1–4, the clutter covariance matrix, C, is required to compute the average interference power against which the target is competing for detection. In the general case, C is a measure of the correlation between the clutter signals found on subapertures i and i′. The components of C, $c_{ii'}^{ll'}$, $l \in [0,N_p-1]$ are

$$c_{ii'}^{ll'} = \left\langle c_{il} \, c_{i'l'}^{*} \right\rangle \tag{109}$$

where <> is the ensemble average operator. In Eqs. 76 and 102, the only statistical parameter is ρ_c. As discussed in Refs. 1–4, the statistics of ρ_c are appropriately described by

$$\left\langle \rho_c[R_c,\varphi_c] \right\rangle = 0 \tag{110}$$

and

$$\left\langle \rho_c[R_c,\varphi_c]\, \rho_c^*[R_{c'},\varphi_{c'}] \right\rangle = \sigma^o[\gamma_c]\, \frac{1}{R_c} \frac{r_s}{r_e}\, \delta[R_c - R_{c'}]\, \delta[\varphi_c - \varphi_{c'}] \qquad (111)$$

where $\delta[x-x']$ is the Dirac delta function. The first expression states that the mean value of the complex reflectivity of a clutter patch is zero. The second expression states that distinct clutter patches are uncorrelated and that the backscattering coefficient of a clutter patch is $\sigma^o[\gamma_c]$.

Using Eqs. 110 and 111 and noting that the statistical independence of the clutter patches causes the cross terms to vanish, Eq. 109 becomes:

$$c_{ii'}^{ll'} = \left[\frac{r_e}{r_s}\right] \int_{R_c} \int_{\varphi_c} \bar{c}_{il}\, \bar{c}_{i',l'}^{*}\, \sigma^0[\gamma_c]\, R_c\, dR_c\, d\varphi_c \qquad (112)$$

Eq. 112 can easily be expanded by replacing $\bar{c}_i[t]$ and $\bar{c}_{i'}[t]$ by their respective values. The expression obtained is rather complicated and not very informative. If frequency hopping is not used, the expanded version of Eq. 112 simplifies considerably. For the NFM case, Eq. 112 is identical to the equation found in Refs. 1–4, provided the second order phase terms are neglected.

2.7 The Thermal Noise Covariance Matrix

In radar systems, the target also has to compete against white thermal noise for

detection. As for clutter, the noise covariance matrix, N, is used to compute the noise interference. Its definition is

$$N[t,\tau] = \left\langle n[t]n^{*}[t+\tau] \right\rangle \tag{113}$$

where τ is the time interval and where n[t] denotes the noise signal. Assuming that the noise is a stationary stochastic process, N becomes independent of t:

$$N[\tau] = \left\langle n[t]n^{*}[t+\tau] \right\rangle \tag{114}$$

As discussed in Ref. 13, the expected value in the expression above is given by the Weiner–Kinchine relation:

$$N[\tau] = \int_{-\infty}^{\infty} S_n[f] \exp[j2\pi f\tau]\, df \tag{115}$$

where f is the frequency and $S_n[f]$ is the autospectral density function of the noise. At the output of a filter of transfer function H[f], $S_n[f]$ relates to the autospectral density function of the white noise at the input of the filter, $S_w[f]$, in the following manner:

$$S_n[f] = S_w[f]\, |H[f]|^2 \tag{116}$$

For white thermal noise, $S_w[f]$ is a constant and N_0 is given by the well known

relationship

$$N_0 = k_B T_s \tag{117}$$

where k_B is the Boltzman constant and T_s is the equivalent system temperature. Using Eq. 59 to compute $H_{NFM}[f]$, replacing into Eq. 116 and using Ref. 11, we find

$$\begin{aligned} N[\tau] &= K_{NFM}^2 N_0 (\tau_g - \tau) \quad \text{for } \tau < \tau_g \\ N[\tau] &= 0 \qquad\qquad\qquad\quad \text{elsewhere} \end{aligned} \tag{118}$$

Replacing τ by $(l-l')\tau_r$ and K_{NFM} by its value (Eq. 60), we obtain

$$N_{ll'} = \left[k_B T_s/\tau_g\right] \delta_{ll'} \tag{119}$$

where $\delta_{ll'}$ is the Kroenecker delta function. Eq. 119 is the well known relation linking the noise power to the system temperature and the bandwidth of the radar signal processor. Finally, assuming that the noise is uncorrelated from one receive phase center to another, Eq. 119 becomes

$$N_{ll'} = \left[k_B T_s/\tau_g\right] \delta_{ll'} \delta_{ii'} \tag{120}$$

Using Eqs. 84 and 85, the equivalent expression for the LFM signal is

$$N_{ll'} = \left[k_B T_s/\sqrt{2q}\right] \delta_{ll'} \delta_{ii'} \tag{121}$$

Again, since $q \propto \tau_c^2$, the noise power is proportional to the bandwidth of the radar signal.

2.8 The Signal–to–Interference Ratio

The point target competes against both clutter and noise for detection. The total interference covariance matrix, Λ, describes the statistical properties of the combined interference. Since the clutter and the noise are statistically independent, Λ is

$$\Lambda = C + N \tag{122}$$

where C and N are respectively the clutter and noise covariance matrices.

Recalling the block diagram of Fig. 2, after analog to digital conversion is performed, a digital signal processor is used to enhance the target signal against the interference. It also extracts some features of the target. This enables the data processor to provide useful information about the target, such as position in space, relative velocity etc. The action of the signal processor is, in the ideal case, a linear filtering operation. Mathematically, the filtering operation is the scalar product of the signal vector by a weight vector, W. The components of W are w_{il}, where i is the receive phase center index and l is the sample number. At the output of the signal processor, the ratio of the target power to the interference power is the Signal–to–Interference Ratio (SIR):

$$SIR = \frac{| S^T \cdot W^* |}{W^\dagger \cdot \Lambda \cdot W} \tag{123}$$

where * is the complex conjugate operation, T is the transpose operation and † is the

complex conjugate and transpose operations. Since S is a function of the velocity of the target, SIR also varies with v_s.

The denominator of Eq. 123 contains the average interference covariance matrix. Hence, SIR is an average value. The approach adopted in this report allows one to obtain the average performance of the radar system without using Monte Carlo techniques.

3.0 NUMERICAL RESULTS

3.1 The Computer Simulation

The computer simulation developed for SBRs in Ref. 4 was modified to apply for the airborne scenario. The main modifications consisted of implementing the equations developed in this work, decoupling the velocity of the radar platform from the satellite orbital dynamics, allowing the aircraft to dive, implementing an air–to–air mode and removing the Earth's rotation since the aircraft navigates with respect to the surface of the Earth. An upcoming report will describe the computer simulation in detail.

3.2 The Baseline Airborne Radar System

Table I describes the baseline Airborne Intercept Radar system. It is a conventional pulse Doppler radar using a Medium PRF (MPRF) waveform (Ref. 14). For the baseline case, the aircraft flies at 500 m/s at an altitude of 5 km.

TABLE III

AIRBORNE INTERCEPT RADAR PARAMETERS

Power	1.0 kW
Pulse Repetition Frequency	9.1 kHz
Compression Factor	13.0
Range Resolution	250 m
Number of Pulses Transmitted	16
Antenna Type	Circular
Antenna Diameter	0.7 m
Aperture Illumination Function	Taylor
Antenna Sidelobe Level	–40 dB
Platform Velocity	500 m/s
Platform Altitude	5 km
Target Altitude	0 m
Cross Section Fluctuations	SW II
Terrain Type	Land
Signal Processing	DFT
Time Domain Weighting	Blackman

In the first example, the radar is in the down–looking mode, attempting to detect a slow–moving target at a range of 10 km. The target is close to the surface of the Earth. The radar transmits an LFM waveform with a compression ratio of 13. After pulse compression, the signal is coherently integrated using the standard FFT with Blackman–Harris weighting. Furthermore, two bursts of pulses are integrated non–coherently to reduce the effect of target scintillation. We assume that the signal

from the target does not fluctuate during coherent integration. The target cross section fluctuations obey the Swerling II model from coherent burst to coherent burst.

Fig. 6 shows the signal–to–interference ratio (SIR) of the radar as a function of the velocity of the target. The dotted line is the detection threshold above which a target is present. Fig. 6 shows that the SIR of the radar is very small when the target is stationary. At low velocity, the signal processor cannot distinguish the target from the clutter on the basis of its Doppler shift. As it goes faster, the Doppler shifted target signal moves away from the spectrum of the mainbeam clutter. Eventually, the SIR exceeds the detection threshold and the target is detectable. In the flat portion of the SIR curve, the clutter is almost completely filtered out and the radar performance is essentially noise limited. In the regions of very low SIR, the radar performance is essentially clutter limited. Because sampled signals are periodic with a period equal to the PRF, the SIR becomes very small again when the target moves at approximately 150 m/s.

Hence for the baseline system, the target is detectable in the following velocity intervals : (–136,–18 m/s) and (15.5,133.5 m/s). This means, for instance, that the radar is unlikely to detect ground vehicles unless they have a radial velocity exceeding 56 km/h. This corresponds to a ground velocity of 65 km/h, assuming an angle of 30^{o} between the velocity of the aircraft and the antenna axis of symmetry. The asymmetry between the positive and the negative detectable velocity interval is attributed to the range–doppler coupling of the LFM waveform.

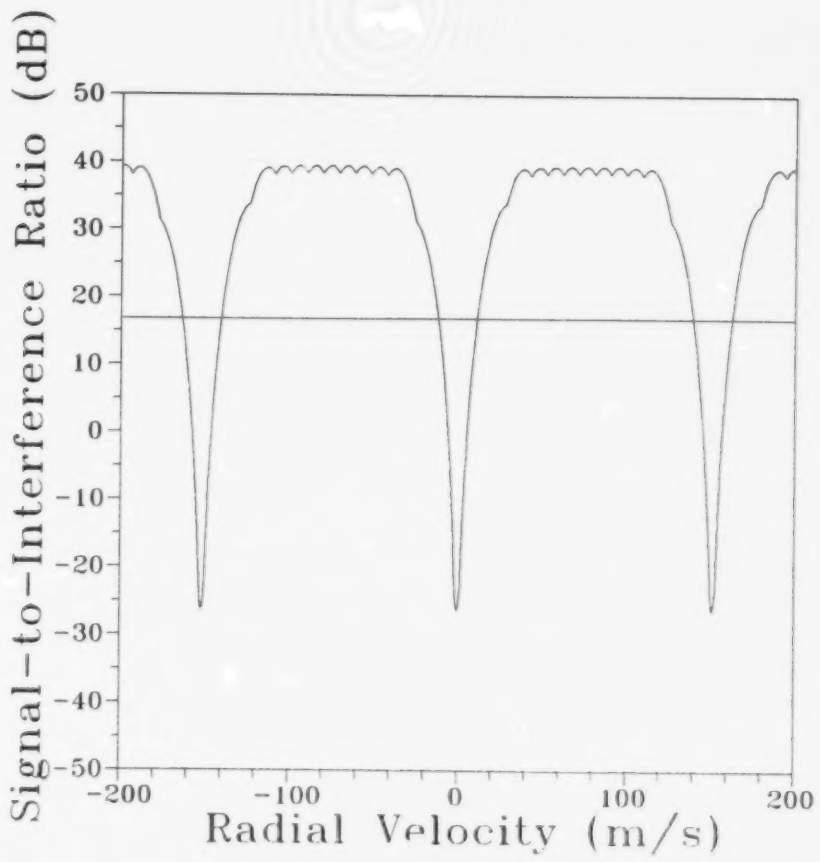

Fig. 6 – The Signal–to–Interference Ratio for the baseline system

There is no trace of an altitude return (the return from terrain directly under the aircraft) in Fig. 6. The altitude of the radar being 5 km and the ambiguous range being 16.48 km, the altitude return occurs beyond a range of 21.48 km. Fig. 7 compares the SIR curves of the baseline case with the one for a range equal to 21.48 km. The altitude return causes the Detectable velocity intervals to practically disappear. Hence, the radar could hardly detect a $10m^2$ target at this range.

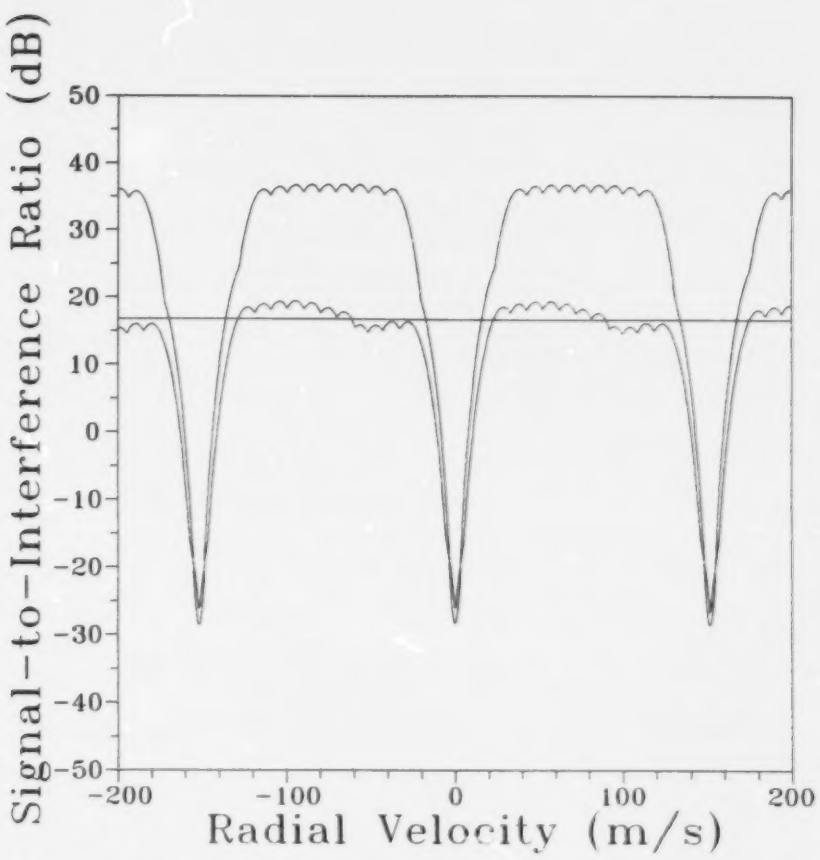

Fig. 7 – SIR of the baseline system with altitude return

Fig. 6 and 7 show that the Intervals of Detectable Velocity shrink as the PRF decreases since the areas of small SIR move closer to each other. A radar with a PRF equal to or lower than 6 kHz would be ineffective in this situation. If the PRF of the radar is too large on the other hand, the range ambiguities increase and the target has to compete with more ambiguous clutter for detection. Thus, a MPRF waveform for which the radar signal is ambiguous in both range and Doppler is a good compromise for the detection of moving targets in the look–down mode.

The performance of the radar with an LFM waveform can be approximated quite closely by using an NFM waveform. In this case, the pulse width is scaled down by the compression ratio and the peak power is scaled up by the same amount. This is shown in Fig. 8 where the SIR for the LFM waveform is compared to the "equivalent" NFM waveform. In the noise limited region, the SNR is approximately 3 dB larger for the NFM case than for the LFM case. This is because the NFM waveform does not require weighting for range sidelobes reduction. The NFM curve is also slightly narrower because it does not have range sidelobes. Since the NFM waveform requires much less computer time, it is often useful to make this approximation.

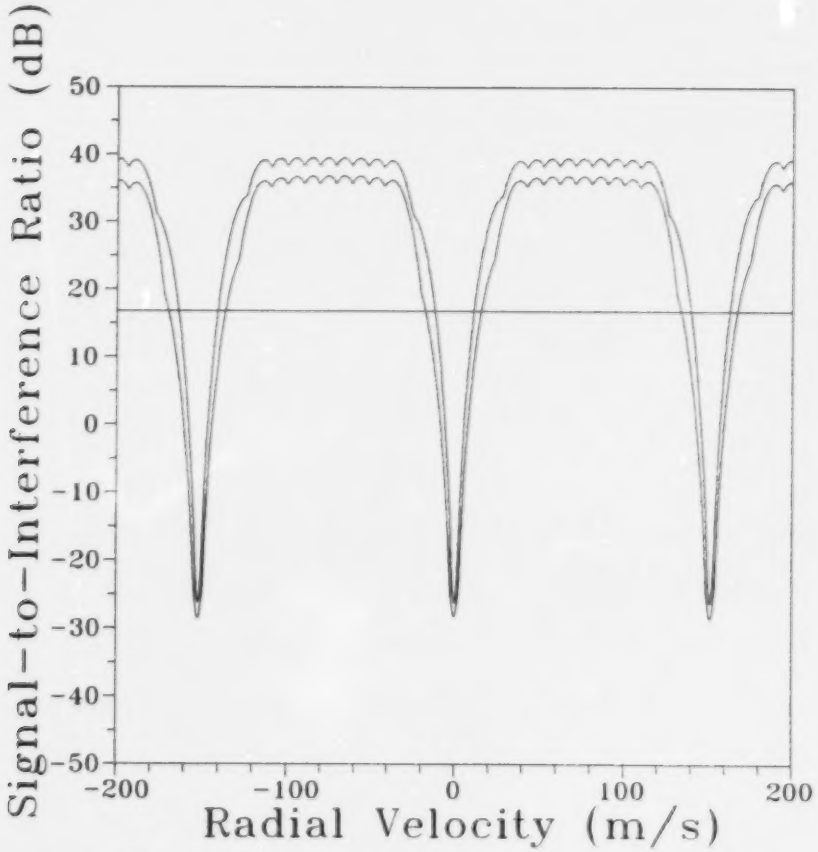

Fig. 8 – SIR of the LFM and the NFM "equivalent" waveform

In an air–to–air encounter, the main beam of the antenna may or may not be pointed toward the surface of the Earth. If it is, Earth clutter penetrates the system and interferes with target detection. However if the main beam of the antenna does not intersect the surface of the Earth, clutter penetrates the radar system only through the sidelobes of the antenna. Except for range gates in which the altitude return is significant, the clutter power is generally quite small and the performance of the system is essentially noise limited. This is shown in Fig. 9 in which the baseline radar system is looking at a target flying at an altitude of 7 km. There is very little clutter interfering with the target. The system is essentially noise limited.

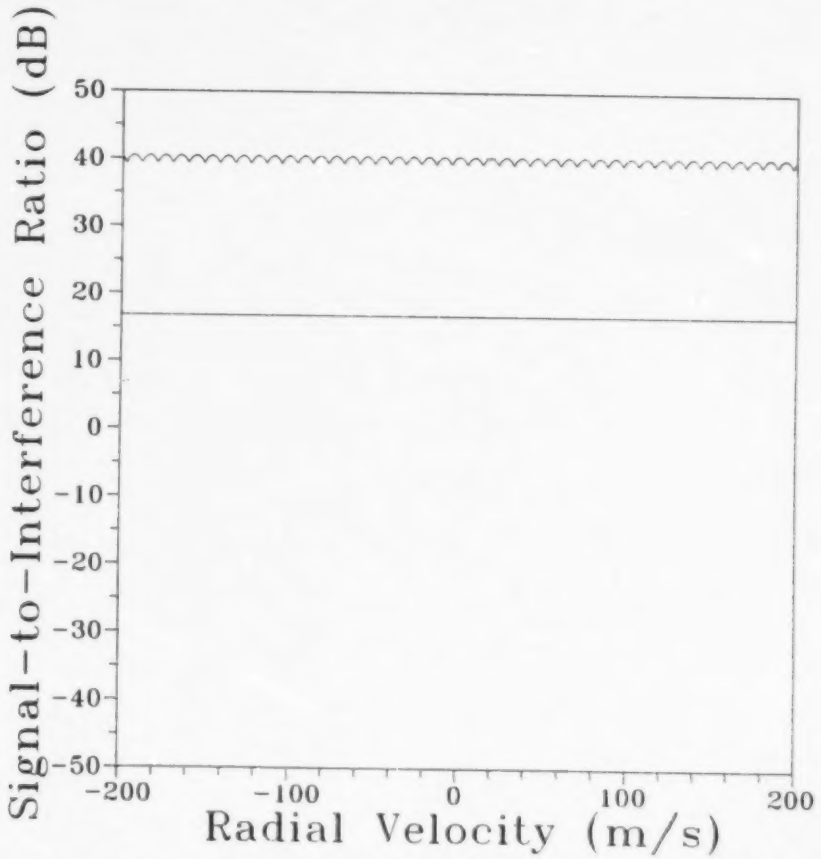

Fig. 9 – SIR of the baseline system for an air–to–air encounter

4.0 CONCLUSION

In this report, we have developed a theory to model the operation of airborne radars. It simulates multiple waveforms and multiple phase centre systems with frequency hopping. It can assess the performance of airborne radar systems and investigate advanced interference suppression techniques. A very interesting feature of the model is its ability to evaluate the average performance of the radar without the use of Monte Carlo techniques. The model has been applied to a baseline Airborne Intercept radar to demonstrate its capability and validity.

5.0 REFERENCES

1. Tam, W. and D. Faubert, "A Theory of Displaced Phase Center Antenna for Space–Based Radars", CRC Report 1409, December 1986.

2. Faubert, D. and W. Tam, "Improvement in the Detection Performance of a Space–Based Radar Using a Displaced Phase Centre Antenna", Digest of the International Symposium on Antenna and Propagation, June 1987, pp 964–967.

3. Tam W. and D. Faubert, "Displaced Phase Center Antenna Clutter Suppression in Space–Based Radar Applications", Digest of the Radar 1987 Conference, October 1987, pp 385–389.

4. Lightstone, L., "A Model of a Displaced Phase Centre Antenna System for Space–Based Radars with Generalized Orbital Parameters and Earth Rotation", Atlantis Scientific Systems Group Report, July 1967.

5. Vant, M.R. and G.E. Haslam, "A Theory of Squinted SAR", CRC Report 1339, November 1980.

6. Skolnik, M.I., "Introduction to Radar Systems", McGraw–Hill Book Company, New York, USA, Second Edition, p. 142, 1980.

7. Klauder, J.R., A.C. Price, S. Darlington and W.J. Albersheim, "The Theory and Design of Chirp Radars", Bell System Technical Journal, Vol. 39, No. 4, pp 745–808, July 1960.

8. Rihaczek, A.W., "Principles of High–Resolution Radar", Mark Resources Inc., Marina del Rey, USA, p 162, 1977.

9. Harris, F.J., "On the Use of Windows for Harmonic Analysis with the Discrete Fourier Transform", Proceedings of the IEE, Vol. 66, No. 1, pp 51–83, January 1978.

10. Nutall, A.H., "Some Windows with Very Good Sidelobe Behaviour", IEEE Transactions on Acoustics, Speech and Signal Processing, ASSP No. 1, pp 84–91, February 1981.

11. Prudnikov, A.P., Yu.A. Brychkov and O.I. Marichev, "Integrals and Series", Gordon and Breach Science Publishers, New York, USA, 1986.

12. Abramowitz, M. and I.A. Stegun, "Handbook of Mathematical Functions", Dover Publications Inc, New York, USA, pp 295–330, 1970.

13. Urkowitz, H., "Signal Theory and Random process", Artech House, Dedham, USA, p 383, 1983.

14. Aronoff, E. and N.M. Greenblatt, "Medium PRF Radar Design and Performance", Hughes Aircraft Company, 1978.

TABLE OF SYMBOLS

Symbol	Description	Units
A_c	Area of an elemental clutter patch	$[m^2]$
A_{dB}	Attenuation at the edge of the bandwidth for the LFM waveform	[dB]
b	LFM frequency sweep rate	$[s^{-2}]$
B	Extent of the LFM frequency sweep	$[s^{-1}]$
c	Speed of light	[m/s]
$c_{ii'}^{ll'}$	An element of the clutter covariance matrix	[W]
$c_i[t]$	The clutter signal for the ith phase center	$[W^{1/2}]$
c_{il}	The sampled clutter signal	$[W^{1/2}]$
C	The clutter covariance matrix	$[W^{1/2}]$
d/2	Distance from T to R_i	[m]
E[t]	Eclipsing function	[–]
Erf[x]	Complex Error function	[–]
Erfc[x]	Complementary Error Function	[–]
f[t]	A general waveform	[–]
g_i^a	Complex directivity of the ith receive phase center	[–]
g_t	Complex directivity of the transmitter	[–]
g_i $[W^{1/2}/m]$	$=K_t K_r g_i^a g^{amp}$	
g^{amp}	Gain of the amplification chain	[–]

h	Altitude of the aircraft	[m]
$h[t]$	Impulse response of a matched filter	[s^{-1}]
$h_{NFM}[t]$	Impulse responses of the matched filter for the NFM waveform	[s^{-1}]
$h_{LFM}[t]$	Impulse response of the mismatched filter for the LFM waveform	[s^{-1}]
$H_c[\omega]$	Transfer function of the compressor	[–]
$H_p[\omega]$	Transfer function of the weighting operation	[–]
$H[t]$	Heavy side step function	[–]
$H[f]$	Transfer function of a filter	[–]
$\hat{i}$	Unit vector along the line joining T to R_i	[–]
i,i'	Receiver phase centre index	[–]
j	$\sqrt{-1}$	[–]
k	Index for the transmitted radar pulses	[–]
k'	Number of complete radar pulses transmitted before reception of the first return from a point target	[–]
k_B	Boltzman constant	[J/K]
K_r	Normalization constant for the received signal	[m^{-1}]
K_t	Normalization constant for the transmit signal	[$W^{1/2}$]
K	$=K_tK_r$	[$W^{1/2}/m$]
K_m	Normalization constant for a matched filter	[s^{-1}]
K_{LFM}	Normalization constant for the LFM waveform	[s^{-1}]
K_{NFM}	Normalization constant for the NFM waveform	[s^{-1}]
l	Index for the received radar pulses	[–]

L_s	Radar system losses	[–]
$n[t]$	Noise signal	[$W^{1/2}$]
$n_{ii'}^{ll'}$	An element of the noise covariance matrix	[W]
N	The noise covariance matrix	[W]
N_o	$=S_W[f]$	[J]
N_p	Number of RF pulses transmitted	[–]
N_p	Number of RF pulses transmitted	[–]
P	Transmitted power	[W]
q	Weighting parameter	[s^2]
r_e	Radius of the earth	[m]
r_s	$=r_e + h$	[m]
$r_s[t]$	Vector describing the location of T_s in the calculation reference frame	[m]
$r_c[t]$	Vector describing the location of C in the calculation reference frame	[m]
$\hat{R}$	Unit vector along the line joining T_s to C	[–]
$\vec{R}[t]$	Vector joining T_s to C	[m]
R	Range from T_s to C	[m]
R_c	Range to a clutter patch	[m]
R_g	Range gate	[m]
$S_n[f]$	Autospectral density function of the noise	[J]
$S_w[f]$	Autospectral density function of white thermal noise	[J]

t	Time	[s]
t_o	Time at which an RF pulse is transmitted from T	[s]
t_c	Time at which the RF pulse reaches C	[s]
t_i	Time at which an RF pulse is received at R_i	[s]
T_s	System temperature	[K]
$u[t]$	The transmitted waveform	$[W^{1/2}]$
$\vec{v}_s[t]$	Velocity of the radar	[m/s]
$\vec{v}_c[t]$	Velocity of the point target	[m/s]
$\vec{V}[t]$	Relative velocity of the radar with respect to a point target	[m/s]
$\vec{V}_r[t]$	Radial velocity of the radar with respect to a point target	[m/s]
$\vec{V}_n[t]$	Normal velocity of the radar with respect to a point target	[m/s]
w_{il}	An element of the linear system weight vector	[–]
W	Weight vector for a linear system	[–]
X	Parameter of the Erf for the LFM waveform	$[s^{-1}]$
$y_i[t]$	The video signal	$[W^{1/2}]$
$y_i^d[t]$	The signal at the output of the circulator	$[W^{1/2}]$
$y_i^r[t]$	The signal at the terminal of the antenna	$[W^{1/2}]$
$y_i^a[t]$	The amplified signal	$[W^{1/2}]$
Y	Parameter of the Erf for the LFM waveform	[s]
$z_i[t]$	The filtered radar signal	$[W^{1/2}]$

$\bar{z}_i[t]$	The portion of $z_i[t]$ which is independent of the target reflectivity	$[W^{1/2}]$
z_{il}	The sampled radar signal	$[W^{1/2}]$
$\alpha[t]$	$=-t + 2R/c + k\tau_r + \tau_f$	[s]
β_k	$2R/C + kt_r + \tau_f$	[s]
γ_c	Antenna grazing angle	[rad]
$\delta[x-x']$	Dirac delta function	[–]
$\delta_{xx'}$	Kroenecker delta function	[–]
δ_0	Coefficient of the zero order term in the expression of Δ_i	[s]
δ_1	Coefficient of the first order term in the expression of Δ_i	[–]
δ_2	Coefficient of the second order term in the expression of Δ_i	$[s^{-1}]$
$\Delta_i[t]$	Propagation delay from T_s to R_i via C	[s]
η,η'	Variable of integration	[s]
η'_{min}	Lower limit of integration	[s]
η'_{max}	Upper limit of integration	[s]
$\theta[\omega]$	Phase of the transfer function of a filter	[rad]
λ_c	Wavelength of the carrier wave	[m]
Λ	The interference covariance matrix	[W]
$\nu[t]$	The complex modulation function of the waveform	[–]
$\mu[t]$	Single pulse modulation function	[–]

$\mu_{NFM}[t]$	Single pulse modulation function for the waveform without frequency modulation	[–]
$\mu_{LFM}[t]$	The single pulse modulation function for the waveform with linear frequency modulation	[–]
$\Pi[t]$	Rectangle function	[–]
ρ	Complex reflectivity of a point target	[m]
ρ_c	Complex reflectivity of a clutter patch	[m]
ρ_c^0	Clutter reflectivity per unit area	[m^{-1}]
σ^0	Clutter backscattering coefficient	[m^2]
τ_p	Width of the uncompressed RF pulse	[s]
τ_c	Width of the compressed radar pulse	[s]
τ_s	Receiver switching time	[s]
τ_d	Group delay in a filter	[s]
τ_f	Portion of the front part of the RF pulse which is eclipsed	[s]
τ_o	Opening time of the receiver	[s]
τ_r	Pulse repetition interval	[s]
τ_l	Duration of the eclipsed RF pulse	[s]
τ_g	Width of a range gate	[s]
τ	$= \tau_l + \alpha[t]$	[s]
$\phi[f]$	Phase of the transfer function of a filter	[rad]
φ_c	Azimuth angle of clutter	[rad]
ω_c	Angular frequency of the carrier wave	[s^{-1}]
ω_{dk}	$=\omega_k + \omega_d$,	[s^{-1}]
ω_k	Pulse to pulse frequency increment	[s^{-1}]

$\omega_{k'}$	Pulse to pulse frequency increment of the receiver center frequency	$[s^{-1}]$
ω_d	Doppler shift of mainbeam clutter	$[s^{-1}]$
ω_{dk}	$=\omega_d+\omega_{k'}$	$[s^{-1}]$
Ω_k	$=\Omega_{ck}\,\delta_1-\Omega_{dk}$	$[s^{-1}]$
Ω_{ck}	$=\omega_k+\omega_c$	$[s^{-1}]$
Ω_{dk}	$=\Omega_k-\omega_{dk}$	$[s^{-1}]$
$\aleph$	Width of a gaussian function	[s]

DOCUMENT CONTROL DATA

(Security classification of title, body of abstract and indexing annotation must be entered when the overall document is classified)

1. ORIGINATOR (the name and address of the organization preparing the document. Organizations for whom the document was prepared, e.g. Establishment sponsoring a contractor's report, or tasking agency, are entered in section 8.)

Defence Research Establishment Ottawa
Department of National Defence
Ottawa, Ontario K1A 0Z4

2. SECURITY CLASSIFICATION (overall security classification of the document. including special warning terms if applicable)

UNCLASSIFIED

3. TITLE (the complete document title as indicated on the title page. Its classification should be indicated by the appropriate abbreviation (S,C,R or U) in parentheses after the title.)

A THEORETICAL MODEL FOR AIRBORNE RADARS (U)

4. AUTHORS (Last name, first name, middle initial)

D. FAUBERT

5. DATE OF PUBLICATION (month and year of publication of document)	6a. NO. OF PAGES (total containing information. Include Annexes, Appendices, etc.)	6b. NO. OF REFS (total cited in document)
NOVEMBER 1989	59	13

7. DESCRIPTIVE NOTES (the category of the document, e.g. technical report, technical note or memorandum. If appropriate, enter the type of report, e.g. interim, progress, summary, annual or final. Give the inclusive dates when a specific reporting period is covered.)

TECHNICAL REPORT

8. SPONSORING ACTIVITY (the name of the department project office or laboratory sponsoring the research and development. Include the address.)

Directorate of Fighter and Trainer Engineering and Maintenance 3-2
National Defence Headquarters
MGen George Pearkes Building
Ottawa, Ontario K1A 0K2

9a. PROJECT OR GRANT NO. (if appropriate, the applicable research and development project or grant number under which the document was written. Please specify whether project or grant)	9b. CONTRACT NO. (if appropriate, the applicable number under which the document was written)
DFTEM 102	

10a. ORIGINATOR'S DOCUMENT NUMBER (the official document number by which the document is identified by the originating activity. This number must be unique to this document.)	10b. OTHER DOCUMENT NOS. (Any other numbers which may be assigned this document either by the originator or by the sponsor)
DREO TECHNICAL REPORT NO. 1017	

11. DOCUMENT AVAILABILITY (any limitations on further dissemination of the document, other than those imposed by security classification)

- (X) Unlimited distribution
- ( ) Distribution limited to defence departments and defence contractors; further distribution only as approved
- ( ) Distribution limited to defence departments and Canadian defence contractors; further distribution only as approved
- ( ) Distribution limited to government departments and agencies; further distribution only as approved
- ( ) Distribution limited to defence departments; further distribution only as approved
- ( ) Other (please specify):

12. DOCUMENT ANNOUNCEMENT (any limitation to the bibliographic announcement of this document. This will normally correspond to the Document Availabilty (11). However, where further distribution (beyond the audience specified in 11) is possible, a wider announcement audience may be selected.)

UNCLASSIFIED

SECURITY CLASSIFICATION OF FORM

13. ABSTRACT (a brief and factual summary of the document. It may also appear elsewhere in the body of the document itself. It is highly desirable that the abstract of classified documents be unclassified. Each paragraph of the abstract shall begin with an indication of the security classification of the information in the paragraph (unless the document itself is unclassified) represented as (S), (C), (R), or (U). It is not necessary to include here abstracts in both offical languages unless the text is bilingual).

This work describes a general theory for the simulation of airborne (or spaceborne) radars. It can simulate many types of systems including Airborne Intercept and Airborne Early Warning radars, airborne missile approach warning systems etc. It computes the average Signal-to-Noise ratio at the output of the signal processor. In this manner, one obtains the average performance of the radar without having to use Monte Carlo techniques. The model has provision for a waveform without frequency modulation and one with linear frequency modulation. The waveform may also have frequency hopping for Electronic Counter Counter Measures or for clutter suppression. The model can accommodate any type of encounter including air-to-air, air-to-ground (look-down) and rear attacks. It can simulate systems with multiple phase centres on receive for studying advanced clutter or jamming interference suppression techniques. An Airborne Intercept radar is investigated to demonstrate the validity and the capability of the model.

14. KEYWORDS, DESCRIPTORS or IDENTIFIERS (technically meaningful terms or short phrases that characterize a document and could be helpful in cataloguing the document. They should be selected so that no security classification is required. Identifiers, such as equipment model designation, trade name, military project code name, geographic location may also be included. If possible keywords should be selected from a published thesaurus. e.g. Thesaurus of Engineering and Scientific Terms (TEST) and that thesaurus-identified. If it is not possible to select indexing terms which are Unclassified, the classification of each should be indicated as with the title.)

Radar, Airborne, Simulation, Pulse Doppler, Theory, Computer Program